Compartmental Models of Cerebral Blood Flow. Analysis Using the 81-keV and 31-keV Photons of ^{133}Xe

W. A. van Duyl, D. Sparreboom, and A. C. W. Volkers

Erasmus University, Rotterdam, and Delft Technological University, Delft, The Netherlands

The clearance of ^{133}Xe from the cerebrum after intra-arterial injection was studied in the pig. A mathematical model, consisting of two exponential terms and a constant, was fitted to decay curves obtained for both the 81-keV and the 31-keV radiation of ^{133}Xe. The corresponding exponential terms for the 31-keV and 81-keV curves were found to differ significantly, implying that the two-compartmental model, based on the partition of the white and gray matter of the brain, is not adequate to describe the clearance process. Other studies have shown that cerebral blood flow is more heterogeneous than the two-compartment model suggests. The discrepancies found here are interpreted as due to the simplification of representing a multiexponential clearance process by means of a two-exponential model.

J Nucl Med 17: 596–602, 1976

Many cerebral bloodflow measurements are based on the clearance of radioactive ^{133}Xe gas from cerebral tissue after bolus injection into the internal carotid artery (*1*). The ^{133}Xe radiation in the tissue is recorded by scintillation detectors placed over the cranium, and the registered radioactivity is usually referred to as the clearance curve. The injected xenon diffuses from the capillaries into the tissue. During clearance the gas re-enters the capillaries and is transported by the blood to the lungs. The clearance from the lungs is highly effective (about 80%), so that the contribution of recirculating xenon to the brain may be considered negligible.

A crucial assumption in the clearance model is that, within the physiologic range of perfusion, the clearance rate is limited by perfusion only, and not by diffusion (*2*). This implies that in tissue of a homogeneous structure the concentration of xenon will be homogeneous and continuously in equilibrium with the concentration of xenon in venous blood. The ratio of the equilibrium concentrations in any tissue and the blood is the tissue–blood partition coefficient. For an arbitrary "compartment" (i.e., any volume of homogeneous tissue), the clearance process is described by a monoexponential function (*3*).

Since cerebral curves are usually fitted to the sum of two exponential functions, two cerebral compartments are being assumed: one consisting of the superficial gray matter, and the other of the deeper white matter. The clearance for this model is represented by

$$r(t) = Ae^{-\alpha t} + Be^{-\beta t},$$

where $r(t)$ is the counting rate as a function of time t; $\alpha = F_g/\lambda_g V_g = f_g/\lambda_g$ is the decay constant of the "fast" exponential component; $\beta = F_w/\lambda_w V_w = f_w/\lambda_w$ is the decay constant of the "slow" exponential component; F_g and F_w are the absolute blood flows in gray and white matter, respectively, within the detected field; V_g and V_w are the volumes of gray and white matter within the detected field; λ_g and λ_w are the partition coefficients for gray and white matter; and f_g and f_w are the specific blood flows in gray and white matter. The coefficients A and B depend on the amount of radionuclide initially present in a compartment; radiation absorption of the tissue;

Received March 21, 1975; revision accepted Jan. 6, 1976.

For reprints contact: W. A. van Duyl, Dept. of Biological and Medical Physics, Erasmus University, P.O. Box 1738, Rotterdam, The Netherlands.

collimator characteristics; and adjustment of the pulse-height selector(s).

In this paper the original two-compartment model of the cerebral clearance process will be criticized from a physical and mathematical point of view. The physical data originate from a series of experiments in which the emission of ^{133}Xe at both 81 keV and 31 keV was studied (*4*).

THEORETICAL CONSIDERATION OF CLEARANCE MEASUREMENTS

With the ^{133}Xe nuclide, 99.95% of the disintegrations involve a transition energy of 81 keV, with 65% of these producing conversion electrons followed by x-ray emissions, predominantly at 31 keV. The other 35% of the disintegrations involve the emission of an 81-keV gamma photon (Fig. 1).

Since radiations at the two energies can be detected separately, two clearance curves can be obtained and used as a check on each other. The linear absorption coefficients for 81-keV and 31-keV radiation in water (*5*), which are assumed to equal those of brain matter, are

$$\mu_{81} = 0.18\ \text{cm}^{-1}; \quad \mu_{31} = 0.33\ \text{cm}^{-1}.$$

The difference of these absorption coefficients imply a corresponding difference between the A and B coefficients of the 81-keV clearance curve and those of the 31-keV clearance curve.

In this investigation of the two-compartment model, two features of the 81-keV and 31-keV clearance curves are of special interest. First, the decay constants are not affected by the absorption coefficient, so that the decay constants (α and β) of corresponding exponential compartments in both clearance curves must be equal. The second feature concerns the ratio of the 31-keV and 81-keV radiations during clearance:

$$\frac{r_{31}}{r_{81}} = \frac{A_{31}e^{-\alpha t} + B_{31}e^{-\beta t}}{A_{81}e^{-\alpha t} + B_{81}e^{-\beta t}}.$$

Each compartment is associated with a typical value of the ratio r_{31}/r_{81}, determined by the detection efficiency for that compartment. This ratio is smaller for the white-matter compartment than it is for the gray matter. However, the ratio r_{31}/r_{81} for the entire cerebrum is a combination of the ratios for the separate compartments, in such a way that the contribution of the "fast" component decreases during clearance. Hence, cerebral clearance studies should yield a decreasing ratio r_{31}/r_{81}, falling eventually to a constant value when the clearance has become monoexponential. Both features of the two-compartment model are independent of the geometry of the tissue compartments.

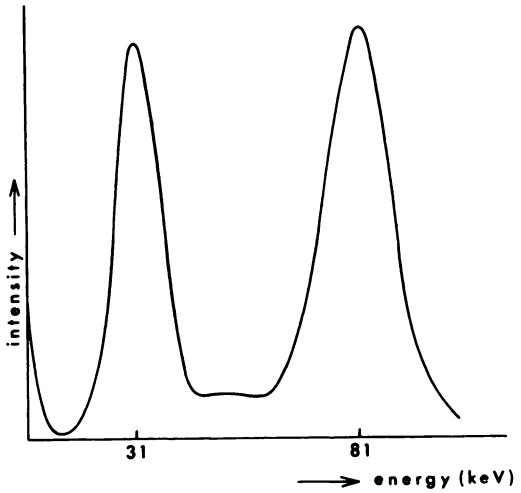

FIG. 1. Energy spectrum of ^{133}Xe, measured with collimated scintillation detector composed of 0.75 × 0.75-in. NaI crystal and photomultiplier tube of outer diameter 19 mm.

In the experimental situation some disturbing phenomena are involved. A consideration of the consequences of scattered radiation and parameter resolution is given in the Appendix.

MATERIALS AND METHODS

In vitro model. A more straightforward test to justify the described features is an experiment with an in vitro model. This model (Fig. 2) consists of two well-stirred perfused compartments, plus a constant plane source on top. The plane source consists of two glass plates of 2 mm thickness, enclosing a 2-mm-thick air space containing some added ^{133}Xe. The plane source is added because we found significant constant background components K_{31} and K_{81} in the analyses of in vivo experiments. The 31-keV and 81-keV clearance curves of this model, after a bolus injection of ^{133}Xe, are analyzed by a digital computer. Figure 2 shows a typical result of such an analysis. Note that, within the accuracy range, the computed decay constants of the corresponding exponential terms of the 31-keV and 81-keV clearance curves are equal. One graph in this figure represents the ratio of the measured 31-keV and 81-keV radiations (r_{31}/r_{81}). If K_{31} is subtracted from r_{31}, and K_{81} from r_{81}, the second graph is obtained, denoted by r'_{31}/r'_{81}. This graph has the theoretically expected course for a two-compartment model.

In vivo experiments. Cerebral bloodflow studies were carried out on Yorkshire pigs (20–35 kg). Besides the similarities between the cardiovascular systems of man and pig (*6*), the large size of a pig's skull helps in placing the scintillation detectors. The pigs were anesthetized by a combination of azaperone (Stresnil) and metomidate (Hypnodil), applied by

infusion into the jugular vein. This type of anesthesia has minimal influence on the cardiovascular system (*7*). The technique was that of Lagerwey (*8*).

The pigs were ventilated through an endotracheal tube shielded with 0.5 mm of lead. To reduce radiation absorption in the cranial bone and to exclude distortion of the clearance curve by extracerebral tissue, a partial window was made in the cranium, and the collimator was fixed into this window (Fig. 3). To avoid loss of cerebrospinal fluid and, hence, a fall of intracranial pressure, a sheet of about 2 mm of cranial bone was left intact. Figure 4 shows the relevant dimensions of the collimator, with the limits of its field of vision. The effects of absorption on the 81-keV and 31-keV radiations were determined by measuring the response to a plane source of ^{133}Xe placed in water at different distances from the collimator face. As seen in Fig. 4, this response is practically a monoexponential function of the distance.

Disturbing effects were reduced by tying off the external carotid artery. About 2 mCi of ^{133}Xe, dissolved in 1 cm^3 of saline, was injected within 1 sec through a thin catheter placed in a common carotid artery through the femoral artery. After the injection the catheter was flushed with saline.

The pulses from the 81-keV and 31-keV photons were selected by separate pulse-height analyzers and recorded on magnetic tape. The recordings were transformed to count-rate functions by counting with preset time intervals of 4 sec. A digital computer was then used to fit a mathematical model consisting of the sum of two or three exponential terms, plus a constant, to each clearance curve. The computer program, adopted from Kirkegaard (*9*), consists of a nonlinear regression analysis based on the least sum of weighted squares of deviations and follows a Marquardt iteration procedure.

RESULTS

Table 1 shows the decay constants of 81-keV and 31-keV clearance curves for a series of experiments, where a model using two exponential components and a constant was fitted to the experimental data. The constants K_{31} and K_{81} are primarily included to account for background radiation. The values of the decay constants indicate rather low cerebral blood-flow values compared to those reported in conscious man (*10*): with $\lambda_g = 0.8$, f_g is about 30 $cm^3/100$ cm^3 tissue/min; and with $\lambda_w = 1.5$, f_w is about 15 $cm^3/100$ cm^3 tissue/min. The eccentricity ξ of the

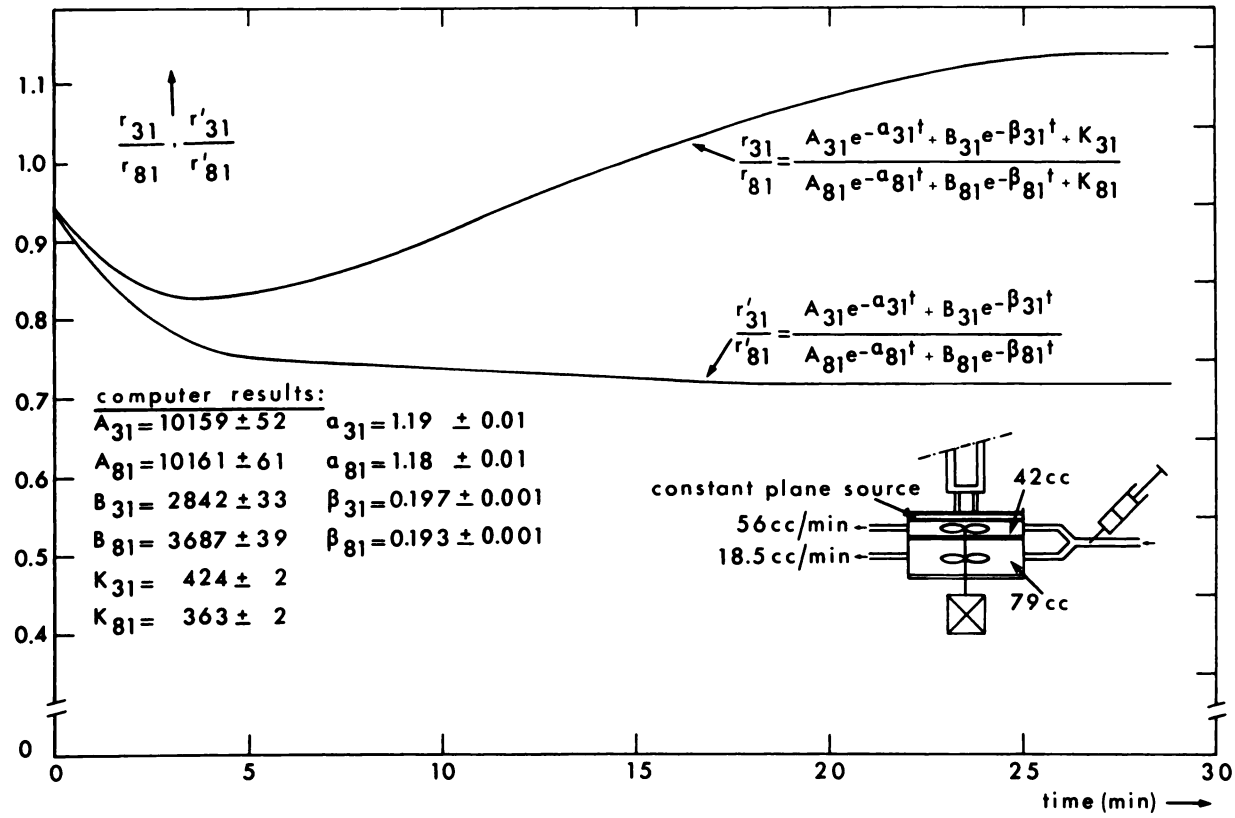

FIG. 2. Results of computer analysis of clearance of in vitro model consisting of two well-stirred compartments and constant plane source.

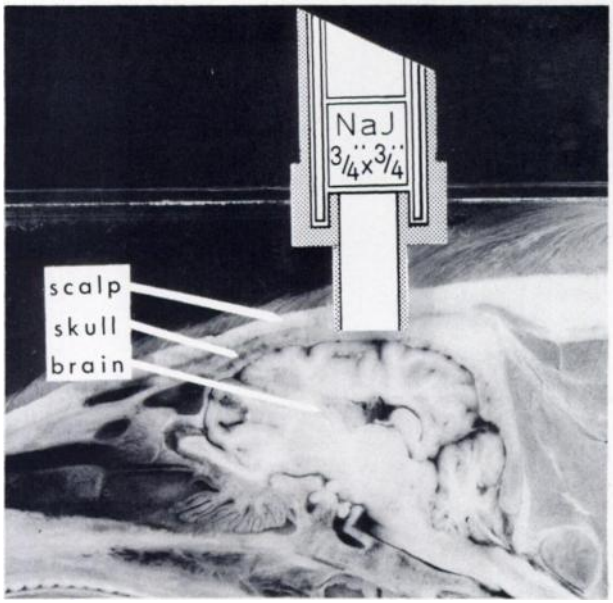

FIG. 3. Arrangement of scintillation detector over cerebrum of pig.

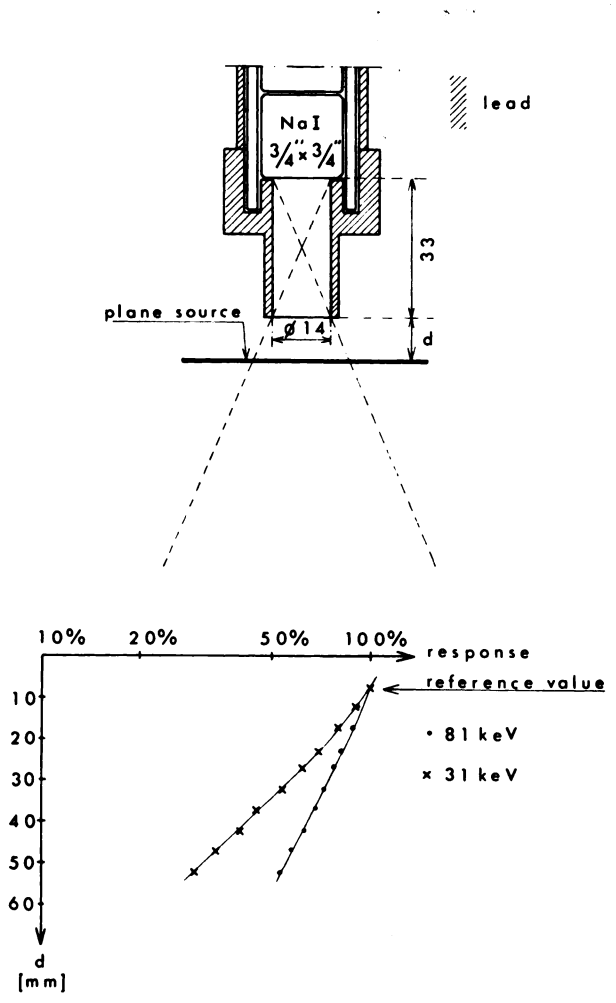

FIG. 4. Dimensions of collimator and its response to 81-keV and 31-keV radiation from ^{133}Xe plane source placed in water.

weighted sum of residual deviations between measured and fitted data of the clearance curve is used to indicate the quality of fit. The residual sum of squares is assumed to have a Gaussian distribution with mean value equal to the number of data, the square root of twice this number being the standard deviation (*11*). In Table 1 these ξ values are shown for both the 31-keV and 81-keV calculations.

After performing the regression analysis with the two-exponential model, a significant lack of fit was found in each clearance curve. This indicates the inadequacy of the applied mathematical model. A careful comparison of the clearance curves with the fitted curves reveals that this lack of fit occurs mainly in the first minute. The computed values for the constants K_{31} and K_{81}, while less than 10% of the coefficients for the "slow" exponential component, are still too high to be ascribed simply to background radiation. In Table 1 the ratio K_{31}/K_{81} is given, in a search for its possible origin.

The decay constants for the 81-keV exponential differ significantly from those of the 31-keV exponential:

$$\alpha_{31} > \alpha_{81}; \quad \beta_{31} > \beta_{81}.$$

This conflicts with the two-compartment theory. Figure 5 shows a plot against time for r'_{31}/r'_{81}, the ratio of the observed clearance data after subtraction of the constants K_{31} and K_{81}. The continuous curve in the plot is obtained from the data for the fitted clearance curves after subtraction of the K constants. Because of the lack of fit in the clearance curves for 81 keV and 31 keV, there is similar lack of fit between the first part of this continuous curve and the dotted points. Note that these curves decrease continuously instead of leveling to a constant value. This means that the tail of the clearance curve does not originate from the clearance of one compartment.

As the main result of this series of experiments, we conclude that the observed 81-keV and 31-keV clearance curves are not compatible with the original two-compartment model.

Results with a modified analysis. In search of a better fit, we compared our experimental curves with those of a model using three exponential terms and a constant (Table 2). Although the fit is now good, the differences between the decay constants are still significant and (in contrast to the two-exponential model) are no longer of constant sign. These differences, however, are probably due mainly to the nonorthogonality of exponential functions. The extreme sensitivity to noise in a three-exponential model makes the determination from experimental data very unreliable (*12,13*).

Since the lack of fit with the two-exponential model

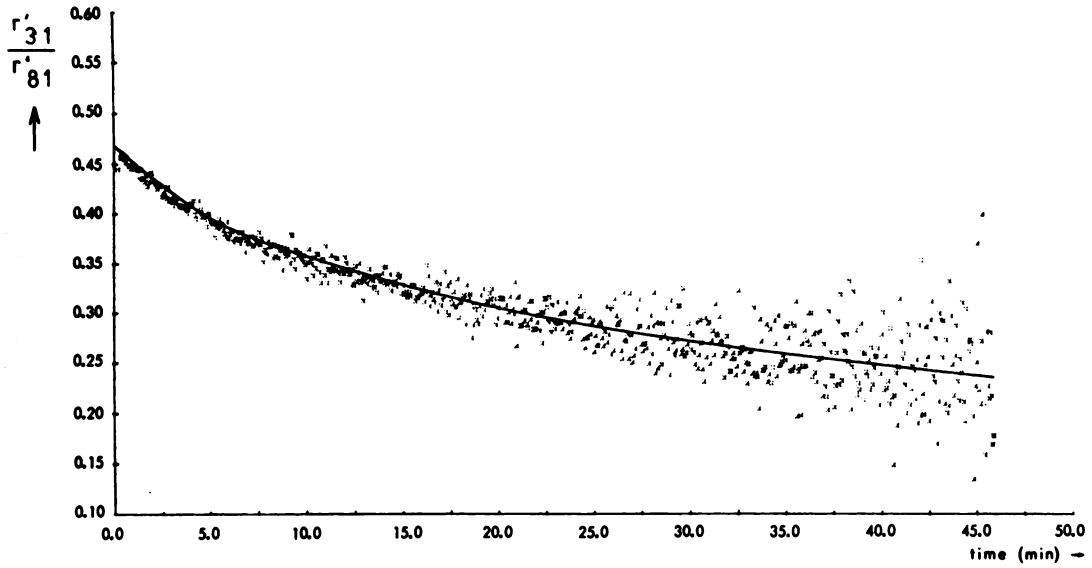

FIG. 5. Plot of r'_{31}/r'_{81} (i.e., the ratio of the 31-keV and 81-keV clearance curves minus constants K_{31} and K_{81}, respectively), obtained from in vivo experiment (Exp. No. 8).

TABLE 1. DECAY CONSTANTS OF 81-keV AND 31-keV CLEARANCE CURVES. FITTED MODEL: A exp (−αt) + B exp (−βt) + K

Exp. No.	α_{81}	β_{81}	ξ_{81}	α_{31}	β_{31}	ξ_{31}	$\frac{\alpha_{31}-\alpha_{81}}{\alpha_{81}}$ (%)	$\frac{\beta_{31}-\beta_{81}}{\beta_{81}}$ (%)	$\frac{K_{31}}{K_{81}}$
1	0.40	0.086	23	0.41	0.102	8	3	16	0.32
2	0.39	0.078	8	0.40	0.087	2	5	11	0.40
3	0.34	0.077	14	0.37	0.089	3	10	16	0.25
4	0.39	0.101	18	0.44	0.119	6	12	16	0.27
5	0.32	0.092	5	0.35	0.100	0.05	8	10	0.25
6	0.39	0.107	17	0.44	0.123	3	13	15	0.22
7	0.37	0.095	11	0.43	0.124	4	17	31	0.19
8	0.33	0.092	21	0.37	0.107	5	11	17	0.25
9	0.35	0.086	23	0.39	0.105	7	13	22	0.22
10	0.33	0.069	13	0.38	0.090	2	14	30	0.23
11	0.37	0.070	15	0.41	0.096	4	12	37	0.20

TABLE 2. DECAY CONSTANTS OF 81-keV AND 31-keV CLEARANCE CURVES. FITTED MODEL: A exp (−αt) + B exp (−βt) + C exp (−γt) + K

Exp. No.	α_{81}	β_{81}	γ_{81}	ξ_{81}	α_{31}	β_{31}	γ_{31}	ξ_{31}	$\frac{\alpha_{31}-\alpha_{81}}{\alpha_{81}}$ (%)	$\frac{\beta_{31}-\beta_{81}}{\beta_{81}}$ (%)	$\frac{\gamma_{31}-\gamma_{81}}{\gamma_{81}}$ (%)
1	3.564	0.331	0.0692	3.4	2.476	0.337	0.0817	1.7	−31	+2	+18
2	0.591	0.282	0.0528	0.6	0.458	0.206	0.0471	0.8	−22	−27	−29
3	4.305	0.316	0.0715	1.0	5.797	0.359	0.0862	0.6	+35	+14	+20
4	0.536	0.206	0.0579	1.6	0.523	0.213	0.0787	0.9	−2	+3	+36
5	12.750	0.316	0.0905	1.1	0.648	0.273	0.0895	0.06	−94	−14	−1
6	0.687	0.264	0.0809	2.0	0.618	0.272	0.0961	1.8	−10	+3	+19
7	2.879	0.347	0.0875	0.7	1.586	0.397	0.1142	0.5	−45	+14	+31
8	1.115	0.257	0.0754	2.6	0.613	0.246	0.0838	0.5	−44	−4	+11
9	0.883	0.261	0.0658	3.4	0.570	0.245	0.0758	1.9	−35	−7	+15
10	0.703	0.248	0.0528	1.8	0.545	0.242	0.0645	1.0	−29	−3	+2
11	0.706	0.276	0.0516	0.2	0.613	0.287	0.0704	0.5	−12	+4	+36

TABLE 3. DECAY CONSTANTS OF 81-keV AND 31-keV CLEARANCE CURVES, IGNORING THE FIRST 70 SEC. FITTED MODEL:
$A \exp(-\alpha t) + B \exp(-\beta t) + K$

Exp. No.	α_{81}	β_{81}	ξ_{81}	α_{31}	β_{31}	ξ_{31}	$\frac{\alpha_{31} - \alpha_{81}}{\alpha_{81}}$ (%)	$\frac{\beta_{31} - \beta_{81}}{\beta_{81}}$ (%)
1	0.33	0.069	2.77	0.35	0.086	1.72	6	25
2	0.37	0.072	3.33	0.39	0.082	3.38	8	14
3	0.32	0.071	1.02	0.36	0.086	0.44	13	21
4	0.36	0.094	10.55	0.41	0.115	3.94	14	22
5	0.32	0.091	2.33	0.33	0.097	1.00	3	7
6	0.35	0.099	6.4	0.40	0.117	0.20	14	18
7	0.35	0.088	0.7	0.41	0.116	0.64	17	32
8	0.29	0.083	3.6	0.33	0.101	0.92	14	22
9	0.31	0.078	3.0	0.36	0.099	4.2	16	27
10	0.31	0.064	3.6	0.36	0.085	0.03	17	33
11	0.34	0.064	5.0	0.38	0.086	0.8	11	34

was found in the first part of the clearance curve, the analyses were repeated with the two-exponential model, this time ignoring data from the first 70 sec (Table 3). The fit looks good, but the discrepancies in the decay constants are of the same order of magnitude as in the original analyses. Thus, the discrepancies cannot be caused by a bad fit.

DISCUSSION

In this series of cerebral bloodflow measurements in the pig, rather low values are found. In another series of experiments in which we used nitrous oxide anesthesia, we found specific bloodflow values in the same range (mean blood pressure, 70–110 mm Hg). Hence, we cannot ascribe our present low values to the anesthesia. We have been unable to find published values for specific cerebral blood flow in the pig.

Our observation time for bloodflow measurement is long compared to other investigators, and because our bloodflow values are less than half the values reported for man, the decay constants are also much smaller. For comparable accuracy, therefore, our experiments needed the longer time.

Recirculation of xenon is more important than is assumed in the idealized clearance process since the tail of the clearance curve may be influenced by recirculation. Unlike many other investigators, however, we included a constant in our mathematical model. Such "constant" radiation might originate from regions that clear very slowly, e.g., sinuses, cerebrospinal fluid, or bone. This supposition is supported by the computed ratio of the constants K_{31}/K_{81}, which indicates that the "constant" source is equivalent to a plane source located at half the depth of the brain. This radiation source may be built up partly by tracer recirculation and partly by release of xenon from poorly perfused areas, such as the cerebrospinal fluid spaces. In our in vitro model we put a constant plane source on top of the two compartments. Its situation, however, is irrelevant: it needs only to provide constant radiation.

The lack of fit of the two-exponential model during the first minute of the clearance curve may be caused by the transit of the tracer through the vascular bed without exchanging with tissue (*14*). It is worth mentioning that a brief initial plateau is often found in the r'_{31}/r'_{81} curve (Fig. 5).

If the first minute of the clearance process is ignored, the clearance curve can be described perfectly well with two exponential terms and a constant. This, however, is not sufficient to justify applying the two-compartment model. The differences in the decay constants of the 31-keV and 81-keV clearance curves show that the clearance process is more complex.

Autoradiographic studies (*15,16*) have shown that cerebral blood flow is more heterogeneous than is assumed in the two-compartment model. A bimodally distributed multiexponential model describes the clearance process better. Furthermore, Reivich et al (*17*) have shown that such a model can be fitted well with two exponential terms. The fitted parameters of that two-exponential model depend on the mean values and the shapes of the modes of the bimodal distribution. Each exponential term refers to a particular region of cerebral tissue. Because of the different absorption coefficients for 31-keV and 81-keV radiation, the coefficients of any exponential term, measured with 31-keV and 81-keV radiation, will depend on the location of that tissue region. This implies that the shape of the distribution function of the multiexponential model is different for the 31-keV radiation and for the 81-keV radiation. In our opinion, this explains the discrepancies found in the

analyses of our 31-keV and 81-keV clearance curves. Our data thus are consistent with heterogeneous cerebral blood flow.

This interpretation indicates the need for measurements of the distribution of cerebral blood flow, which can be determined with radioactive microspheres that become trapped in the capillaries (*17*). Results of such a study will be published in a subsequent paper.

Finally, we think it worthwhile to look for a model in which the data from the 31-keV and 81-keV clearance curves are combined, in order to get an idea about the flow distribution in the depth of the cerebrum. In contrast to the autoradiographic technique, here information about the flow distribution is obtained without killing the animal.

APPENDIX

Contribution of scattered radiation. The Compton scattered radiation from the 81-keV photons contributes to the count rate in the 31-keV energy range. We assume that this contribution is proportional to the intensity of the detected 81-keV radiation:

$$\Delta r_{31} = c r_{81}.$$

Combining this with

$$r_{81} = A_{81}e^{-\alpha t} + \beta_{81}e^{-\beta t} + K_{81},$$

we get

$$\Delta r_{31} = cA_{81}e^{-\alpha t} + cB_{81}e^{-\beta t} + cK_{81},$$

so that:

$$r_{31} = (A_{31} + cA_{81})e^{-\alpha t} + (B_{31} + cB_{81})e^{-\beta t} + (K_{31} + cK_{81}).$$

Hence, if the above assumption of proportionality holds, the decay constants are not affected.

Parameter resolution in exponential models. Because of the nonorthogonal properties of exponential functions, there is an interdependency of the computed parameters expressed in their cross-correlation coefficients. In our analysis the cross-correlation coefficients of A with $-\alpha$ and of B with $-\beta$ turned out to be negative. Since $A_{81}/B_{81} < A_{31}/B_{31}$, these cross-correlation coefficients predict a probability that $\alpha_{31} < \alpha_{81}$ and $\beta_{31} < \beta_{81}$. In other words, the differences found experimentally are even reduced, albeit slightly, by the cross-correlation effects.

ACKNOWLEDGMENTS

This work was done under the supervision of G. van den Brink and Y. J. Kingma, to whom we are grateful for their stimulating interest. We thank R. P. Forsyth for reading the manuscript and N. J. Dijkdrenth-Duijzend for skilled typing.

REFERENCES

1. LASSEN NA, INGVAR DH: Regional cerebral blood flow measurement in man. *Arch Neurol* 9: 615–628, 1963

2. KETY SS: The theory and applications of the exchange of inert gas at the lungs and tissues. *Pharmacol Rev* 3: 1–41, 1951

3. KETY SS: Measurement of local circulation within the brain by means of inert, diffusible tracers: Examination of the assumptions and possible sources of error. In *Proceedings of the International Symposium on Regional Cerebral Blood Flow*, Ingvar DH, Lassen NA, eds. Copenhagen, Munksgaard, 1965, pp 20–23

4. VAN DUYL WA, MECHELSE K, SPARREBOOM D, et al: Interpretation of differences between "81-keV" and "31-keV" decay curves registrated during clearance of Xe-133 in cerebral tissue of the pig. In *Proceedings of the International Symposium on Cerebral Circulation and Metabolism*, Langfitt W, McHenry LC, Reivich M, Wollman H, eds. New York, Springer, 1975, pp 409–412

5. HINE GJ, BROWNELL GL: *Radiation Dosimetry*. New York, Academic, 1956, p 83

6. DOUGLAS WR: Of pigs and men and research, a review of applications and analogies of the pig, *sus scrofa*, in human medical research. *Space Life Sci* 3: 226–234, 1972

7. Janssen Pharmaceutica: The potentiated anaesthesia in pig with R1929 and R7315. Technical Report No. 9, Belgium, 1968

8. LAGERWEY E: Anaesthesia in swine for experimental purposes. Thesis (in Dutch), Utrecht, 1973

9. KIRKEGAARD P: A fortran IV version of the sum of exponential square code exposum. Rapport Risö-M-1279, Research Establishment Risö, Danish Atomic Energy Commission, September, 1970

10. INGVAR DH, CRONQUIST S, EKBERG R, et al: Normal values of regional cerebral blood flow in man, including flow and weight estimates of grey and white matter. A preliminary summary. *Acta Neurol Scand Suppl* 14: 72–78, 1965

11. DRAPER N, SMITH H: *Applied Regression Analyses*. New York, Wiley, 1967, pp 63–86

12. MYHILL J: Investigation of the effect of data error in the analysis of biological tracer data. *Biophys J* 7: 903–911, 1967

13. MYHILL J: Investigation of the effect of data error in the analysis of biological tracer data from three-compartment systems. *J Theor Biol* 23: 218–231, 1969

14. VAN DUYL WA, VOLKERS ACW, SPARREBOOM D: Measurement of specific cerebral blood flow of the pig based on the radio-active clearance technique with Xe-133. In preparation

15. LANDAU WM, FREYGANG WH, ROWLAND LP, et al: The local circulation of the living brain: Values in the unanesthetized and anesthetized cat. *Trans Am Neurol Assoc* 80: 125–129, 1955

16. REIVICH M, JEHLE J, SOKOLOFF L, et al: Measurement of regional cerebral blood flow with antipyrine C-14 in awake cats. *J Appl Phys* 27: 296–300, 1969

17. REIVICH M: Observations on exponential models of cerebral clearance curves. In *Research on Cerebral Circulation*, Meyer JS, ed. Salzburg, Springfield, 1969, pp 135–144